MiRNA-mRNA integrative analysis reveals epigenetically regulated and prognostic miR-103a with a role in migration and invasion of carboplatin-resistant ovarian cancer cells that acquired mesenchymal-like phenotype

Pernar Kovač, Margareta; Tadić, Vanja; Kralj, Juran; Milković Periša, Marija; Orešković, Slavko; Babić, Ivan; Banović, Vladimir; Zhang, Wei; Culig, Zoran; Brozović, Anamaria

Source / Izvornik: **Biomedicine & Pharmacotherapy, 2023, 166**

Journal article, Published version
Rad u časopisu, Objavljena verzija rada (izdavačev PDF)

https://doi.org/10.1016/j.biopha.2023.115349

Permanent link / Trajna poveznica: https://urn.nsk.hr/urn:nbn:hr:105:807947

Biomedicine & Pharmacotherapy 166 (2023) 115349

Contents lists available at ScienceDirect

Biomedicine & Pharmacotherapy

journal homepage: www.elsevier.com/locate/biopha

MiRNA-mRNA integrative analysis reveals epigenetically regulated and prognostic miR-103a with a role in migration and invasion of carboplatin-resistant ovarian cancer cells that acquired mesenchymal-like phenotype

Margareta Pernar Kovač [a], Vanja Tadić [a], Juran Kralj [a], Marija Milković Periša [b,c], Slavko Orešković [d], Ivan Babić [d], Vladimir Banović [d], Wei Zhang [e], Zoran Culig [f], Anamaria Brozovic [a,*]

[a] Division of Molecular Biology, Ruđer Bošković Institute, Bijenička cesta 54, HR-10000 Zagreb, Croatia
[b] University Hospital Centre Zagreb, Department of Pathology and Cytology, Petrova ulica 13, HR-10000 Zagreb, Croatia
[c] University of Zagreb, School of Medicine, Institute of Pathology, Šalata 10, HR-10000 Zagreb, Croatia
[d] Department of Obstetrics and Gynecology, University Hospital Center Zagreb, Petrova 13, HR-10000 Zagreb, Croatia
[e] Department of Engineering Mechanics, Dalian University of Technology, Linggong Road 2, 116024 Dalian, China
[f] Department of Urology, Medical University of Innsbruck, Anichstrasse 35, A-6020 Innsbruck, Austria

ARTICLE INFO

Keywords:
Drug resistance
Ovarian cancer
MicroRNA
Epithelial-mesenchymal transition
Biomarkers
Epigenetic regulation

ABSTRACT

Background: DNA methylation, histone modifications, and miRNAs affect ovarian cancer (OC) progression and therapy response.
Purpose: Identification of epigenetically downregulated miRNAs in drug-resistant OC cell lines with a possible role in drug resistance and/or drug-induced mesenchymal-like phenotype.
Methods: MiRNA profiling was performed on parental and carboplatin-resistant OC cells, MES-OV and MES-OV CBP. RT-qPCR validation, epigenetic modulation and other CBP-resistant OC cell lines were used to select miRNAs of interest. The integration of miRNA-predicted target genes and differentially expressed genes (DEGs), pathway and functional analysis were used for forecasting their biological role. Data mining was performed to determine their possible prognostic and predictive values.
Results: MiRNA profiling revealed 48 downregulated miRNAs in OC cells whose drug sensitivity and metastatic potential were impacted by epigenetic modulators. Of the fourteen selected, nine were validated as changed, and seven of these restored their expression upon treatment with epigenetic inhibitors. Only three had similar expression patterns in other OC cell lines. MiRNA-mRNA integrative analysis resulted in 56 target DEGs. Pathway analysis revealed that these genes are involved in cell adhesion, migration, and invasion. The functional analysis confirmed the role of miR-103a–3p, miR-17–5p and miR-107 in cell invasion, while data mining showed their prognostic and predictive values. Only miR-103a–3p was epigenetically regulated at the constitutive level.
Conclusion: High throughput miRNA and cDNA profiling coupled with pathway analysis and data mining delivered evidence for miRNAs which can be epigenetically regulated in drug-resistant, mesenchymal-like OC cells as possible markers to combat therapy-induced short overall survival and tumor metastatic potential.

1. Introduction

The death rate of ovarian cancer (OC) is the highest among malignancies that affect the female reproductive tract. The high-grade serous OC (HGSOC) subtype predominates in the clinical setting and is responsible for a disproportionate share of OC fatalities. For most patients, OC is detected when the disease has already spread in the peritoneum and other organs, classified as advanced stages of IIb to IV, according to The International Federation of Gynecology and Obstetrics classification [1,2]. The development of malignant ascites is particularly

* Correspondence to: Ruđer Bošković Institute, Division of Molecular Biology, Bijenička cesta 54, HR-10000 Zagreb, Croatia.
E-mail address: brozovic@irb.hr (A. Brozovic).

https://doi.org/10.1016/j.biopha.2023.115349
Received 26 April 2023; Received in revised form 7 August 2023; Accepted 19 August 2023
Available online 25 August 2023

common with the HGSOC subtype, with free-floating cancer cells dispersed from the primary tumor, leading to intraperitoneal metastases [3]. The aggressiveness mechanisms of OC, including the formation of metastases, build-up of ascitic fluid, therapy resistance and therapy-induced metastatic progression, need to be clarified, providing new targets for more effective disease control and treatment.

It is known that drug treatment might trigger epithelial-mesenchymal transition (EMT), a process involved in tumor cells' metastasis. Drug-induced EMT is described as an important factor in tumor spreading and failure of the therapy [4,5]. Despite a progressive increase in data regarding the correlation between the occurrence of drug resistance and EMT in tumor cells [6], many details about the connection between these two phenomena are still unknown.

MicroRNAs (miRNAs) are short non-coding RNA sequences described mostly as regulators of different genes at the post-transcriptional level. Dysregulation of miRNA expression has an impact on cancer progression since miRNAs regulate many oncogenes and tumor suppressor genes [7–9]. Moreover, many reports emphasize the importance of epigenetic regulation as a factor that influences changes in miRNA expression [10]. For example, it is known that members of the miRNA-200 family are epigenetically regulated [11] and involved in drug resistance and EMT [4,12].

Epigenetic regulation is crucial in tumor initiation and development. DNA methylation and histone modifications are epigenetic alterations that occur in the cell and are implicated in OC pathogenesis [13]. Several epigenetically regulated miRNAs have been identified in OC facilitating peritoneal metastasis, aggressiveness and drug resistance [14,15].

In this study, we focused on epigenetically regulated miRNAs differing in expression between cells with the drug-induced acquired mesenchymal-like phenotype (AMP) and parental OC cells. For that purpose, the parental MES-OV and carboplatin (CBP)-induced AMP MES-OV CBP cell lines were used to identify miRNAs that could impact cancer spread in response to the therapy. Upon determination of potentially epigenetically regulated miRNAs, additional narrowing of the obtained candidates list was accomplished by using two other AMP OC cell models, OVCAR-3 CBP and SK-OV-3 CBP and their appropriate parental cell lines. Data from high-throughput miRNA and mRNA microarray profiling were analyzed and coupled with the Kyoto Encyclopedia of Genes and Genomes (KEGG) pathway enrichment analysis that led to the identification of biological pathways regulated by three miRNAs of interest. Functional analyses were performed, defining their role in cell metastatic potential. We assessed the methylation and chromatin status of the promoter sequences of miR-103a–3p, miR-107 and miR-17–5p constitutively and upon treatment with epigenetic inhibitors. The prognostic value of those miRNAs was also determined.

2. Materials and methods

2.1. Chemicals

Carboplatin was purchased from Sigma Aldrich (USA), dissolved in water and stored at −20 °C. The 5-Aza-2'-Deoxycytidine (5-aza; decitabine; Sigma Aldrich) was dissolved in acetic acid:water (1:1) and Trichostatin A (TSA; Sigma Aldrich) was dissolved in water. Both inhibitors were kept at −20 °C upon reconstitution.

2.2. Cell lines

The human ovarian carcinoma MES-OV and OVCAR-3 GFP cell lines were obtained from Prof. Sikic (Stanford University, USA). SK-OV-3 cell line was purchased from American Type Culture Collection (ATCC; USA). The establishment of human ovarian carcinoma variants resistant to CBP (MES-OV CBP, OVCAR-3 GFP CBP and SK-OV-3 CBP) was described previously [16]. Briefly, CBP-resistant variants were obtained by consecutive 72-h treatments of parental either MES-OV, OVCAR-3 or SK-OV-3 cells with increasing concentrations of CBP, finally reaching the clinically relevant dose of 25 μM. All cell lines acquired stable resistance to CBP and mesenchymal-like phenotype [16] and Fig. S1. The cells were grown in McCoy's 5 A medium supplemented with 10% fetal bovine serum (FBS) (Gibco BRL Life Technologies, USA) and cultured in a humidified atmosphere of 5% CO_2 at 37 °C.

2.3. Cell viability

The cell viability was determined using the Alamar Blue colorimetric assay [17] (Sigma-Aldrich). The absorbance of resorufin was measured using a microplate reader (Awareness Technology Inc., USA). Mass survival assay was used to measure cell survival upon treatment with a combination of epigenetic inhibitors and CBP. Cells were seeded in 6-well plates and 24 h later co-treated with 1 μM 5-aza or 33.3 nM TSA or their combination, and different concentrations of CBP for 72 h (medium with freshly added drugs was changed every 24 h). The treatment effect was visualized by cells' fixation with cold methanol and staining with crystal violet. ImageJ was used to measure the intensity of color and the area under the curve (AUC) proportional to cell proliferation. All experiments were repeated at least three times.

2.4. Total RNA isolation, miRNA array and data processing

Total RNA for microarray was isolated from the sub-confluent growing cells 48 h after seeding. After trypsinization, cells were washed in PBS and pelleted by centrifugation for 5 min at 1200 rpm. Total RNA was isolated with AllPrep DNA/RNA Mini Kit (Qiagen) according to the modified manufacturer's protocol. The miRCURY LNA RT kit (Qiagen) was used for cDNA synthesis. Human panel I+II, V5, miRCURY LNA miRNA miRNome PCR Panel (Qiagen) were used for the miRNA array, covering 752 miRNAs. MiRNAs of interest were filtered by a fold change > 1.25 and < 0.8. Two biological replicates were used for the miRNA microarray assay. MiRBase was used to determine chromosome distribution and identify clustered miRNAs [18]. The bioinformatics data analysis of the mRNA microarray of MES-OV and MES-OV CBP (indicated as MES-OV CBP8) cell lines is described in Kralj et al. [16].

2.5. Quantification of miRNA expression using RT-qPCR

Total RNA for reverse transcription-quantitative PCR (RT-qPCR) validation of miRNA expression was isolated from the sub-confluent growing cells 48 h after seeding with AllPrep DNA/RNA Mini Kit (Qiagen) according to the modified manufacturer's protocol. For the functional analyses, total RNA was isolated either after cell treatment with a combination of 1 μM 5-aza and 33.3 nM TSA or after transfection with mimics using an RNeasy Mini Kit (Qiagen, Germany). For RT-qPCR analysis, 1 μg of total RNA was used for the first-strand cDNA synthesis by using the miScript II RNA Kit (Qiagen) according to the manufacturer's protocol. The expression of specific miRNAs was detected by using SYBR Green dye (miScript SYBR Green PCR Kit, Qiagen) and miScript Primer Assay (Qiagen), with *RNU6* (Qiagen) as an internal control. Fold change of expression was calculated as $2^{-\Delta\Delta Ct}$. The amplification efficiency was determined by serial dilutions of the template. All reactions were performed in triplicate. Dissociation curves were recorded after each run to confirm primer specificity.

2.6. Wound healing (scratch) assay

Cells were seeded in 24-well plates in two replicates. The growing medium was removed a day after, and a starvation medium (McCoy's 5 A medium with 2% FBS) was applied for 24 h to stop proliferation after which three precise scratches were made with a 20 μL sterile pipette tip. Cells were washed twice with PBS, and a standard culture medium was added. Cells were watched and photographed ($n = 12$) on a marked site

immediately (0 h) and after 6 h by bright-field microscope (Olympus BX 51, Olympus Lifescience Ltd., USA). Cell-free areas were measured by ImageJ software (National Institute of Health, USA). The wounding area after 6 h was compared to the area at time point 0 h, expressed as a percentage of migrated cells and plotted as folds of control.

2.7. Cell invasion assay

The desired number of trans-well inserts coated with 40 μL of Matrigel® (Corning, USA) were prepared and inserted into wells of a 24-well plate. Cells were trypsinized, washed three times with culture media without FBS, and re-suspended in the same media. The gelled Matrigel® was then washed with warm FBS-free culture media, the same number of cells was added, and the trans-well inserts were transferred into the wells filled with culture media with FBS. Cells were incubated for 22 h at 37 °C. Trans-well inserts were removed from 24-well plates and gently scraped with a cotton swab to remove the Matrigel® and non-invaded cells from the upper side of the membrane. Cells on the lower side of the membrane were then stained with 1% crystal violet in PBS upon fixation in 3.7% paraformaldehyde. Invaded cells were photographed using a bright-field microscope (Olympus BX 51, Olympus Lifescience Ltd.). The area covered by invaded cells was measured by ImageJ software as an area under the curve (AUC), normalized to control, and plotted as a fold of control.

2.8. Methylation-specific PCR (MSP) assay design

For the MSP assay design, CGIs located near the transcription start site within the promoter sequence of the host gene of each miRNA were selected. For that purpose, UCSC Genome Browser and its CGI prediction track in the current human reference genome assembly (GRCh38/hg38) and the ENCODE regulation track showing the active chromatin segments were used [19,20]. Nucleotide sequences of the selected CGIs within promoter regions of the miRNA host genes were retrieved using the UCSC Table Browser tool and used as input sequences for the MethPrimer software [21,22]. Primers were selected from the MethPrimer, taking into account at least 2 CpG sites per primer, one of them being within the last three nucleotides on the 3' end, the same CpG sites in methylated and unmethylated primer pairs and similar annealing temperatures. Each primer pair was checked for its specificity using the completely methylated or completely unmethylated bisulfite-converted EpiTect Control DNAs (Qiagen), and EpiTect unconverted, unmethylated human genomic DNA (Qiagen). Primers for miR-103a–3p and miR-17–5p host gene promoters were designed following the described procedure. The primers for miR-107 promoter correspond to those used by Lee et al. [23] (Table 1). The positions of PCR products amplified by the selected primers which analyzed methylation of CGI 81 (MSP-miR-103a–3p assay), CGI 252 (MSP-miR-17–5p assay) and CGI 99 (MSP-miR-107) in GRCh38/hg38 are indicated in Fig. S1.

2.9. Analysis of miRNA promoter methylation status using MSP

Cells were treated with the combination of 1 μM 5-aza, 33.3 nM TSA for 72 h (medium with freshly added drugs was changed every 24 h). Cells were then trypsinized, washed in PBS and pelleted by centrifugation for 5 min at 1200 rpm. DNA was isolated by DNeasy Blood & Tissue Kit (Qiagen) and subjected to bisulfite conversion with EZ DNA Methylation-Gold Kit (Zymo Research, USA). The 25 μL MSP reactions contained PyroMark Master Mix (Qiagen), CoraLoad Concentrate (Qiagen), 200 nM of each, forward and reverse primer, and 500 ng of bisulfite-converted DNA. The thermal cycling included an initial step at 95 °C for 15 min followed by 45 cycles of 30 s at 95 °C, 30 s at a specific annealing temperature (Ta) for each fragment, and 30 s at 72 °C. Following the last cycle, PCR products were incubated for 10 min at 72 °C. The MSP reactions were run in Veriti™ 96-Well Fast Thermal Cycler (Thermo Fisher Scientific-Applied Biosystems). Amplified PCR products were loaded onto 2% agarose gels stained with Midori Green Advance DNA dye (Nippon Genetics, Japan) along with a 100 bp DNA ladder (New England Biolabs, USA) and electrophoresed for 45 min at 50 V in 1x TAE buffer.

Table 1
Primers for methylation-specific polymerase chain reactions.

Primer name	Sequence	Ta	Product size (bp)
103a–3p-MetF	GT**C**GT**C**GTATTGAGAAATAGTT**C**GT	52 °C	200
103a–3p-MetR	TCTAC**G**AAAACTAAAAAACCTC**G**AA		
103a–3p-UnMetF	GTTGTTGTATTGAGAAATAGTTTGT	50 °C	200
103a–3p-UnMetR	TCTAC**A**AAAACTAAAAAACCTC**A**AA		
17–5p-set1-MetF	**C**GTTTTTAGAATAAAG**C**GG**C**	48 °C	146
17–5p-set1-MetR	**G**TACAAAATTTAAAAAACC**G**C**G**A		
17–5p-set1-UnMetF	GTTAAAGTGTTTTTAGAATAAAGTGGTG	48 °C	156
17–5p-set1-UnMetR	C**A**TACAAAATTTAAAAAACC**A**C**A**AA		
17–5p-set2-MetF	**C**GTTTTTAGAATAAAG**C**GG**C**	42 °C	137
17–5p-set2-MetR	**G**TACAAAATTTAAAAAACC**G**C**G**A		
17–5p-set2-UnMetF	GTTAAAGTGTTTTTAGAATAAAGTGGTG	50 °C	145
17–5p-set2-UnMetR	C**A**TACAAAATTTAAAAAACC**A**C**A**AA		
107-MetF	TGTGTAGTAGTT**C**GTTTATAG**C**	48 °C	218
107-MetR	**G**ACTCTAC**G**ACTACTAAATC**G**		
107-UnMetF	TGTGTAGTAGTTTGTTTATAGTG	54 °C	220
107-UnMetR	CC**A**ACTCTAC**A**ACTACTAAATC		

*analyzed CpG sites are underlined

2.10. Cleavage under targets and release using nuclease (CUT&RUN)-qPCR assay

After 72 h of treatment with 1 μM 5-aza and 33 nM TSA, CUT&RUN (CUT&RUN Assay Kit, Cell Signaling Technology, USA) was performed according to the manufacturer's instructions. Briefly, 100,000 cells for each sample were washed, bound to Concanavalin A magnetic beads and permeabilized with a digitonin-based buffer prior to antibody binding. The following antibodies were used in the assay: Acetyl-Histone H3 (Lys27) (D5E4) XP® Rabbit mAb, Tri-Methyl-Histone H3 (Lys4) (C42D8) Rabbit mAb and Rabbit (DA1E) mAb IgG XP® Isotype Control (Cell Signaling Technology). Antibody-bound DNA was fragmented with pAG-MNase and purified using DNA Purification Buffers and Spin Columns (ChIP, CUT&RUN) (Cell Signaling Technology). DNA obtained from the CUT&RUN assay was amplified using Power SYBR Green PCR Master Mix (Thermo Fisher Scientific) with the AB7300 Real-Time PCR System (Applied Biosystems, Thermo Fisher Scientific). The following primer sets were used for miR-103a promoter region: forward 5′-ACTGCATGCACGTACGTTTG-3′ and reverse 5′-GTGTCCTTGAAATGC CGGTG-3′; for miR-107 promoter region: forward 5′-GGCTCAGG-CAAAGACCTGTA-3′ and reverse 5′-CTGCACAGAGTAGGTTCCCG-3′ and for miR-17–5p promoter region: forward 5′-GAAGATGGTGGCGGC TACTC-3′ and reverse 5′-ACAACAGGTTTCCCTCCGTC-3′. The Percent of Input (PI) for immunoprecipitated DNA (IP) of each sample was calculated using the formula $PI = 100\% \times 2^{(C[T]\ 100\%Input\ Sample\ -\ C[T]\ IP\ Sample)}$, where C[T] is the average threshold cycle of qPCR. Sample Normalization Spike-In DNA and Sample Normalization Primer Set were used for adjustment of signals using the respective normalization factors (NF) for qPCR calculated using the formula $NF = 2^{(C[T]\ Selected\ IP\ Sample\ -\ C[T]\ Other\ IP\ Sample)}$. The sample with the lowest C[T] value for the Sample Normalization Primer Set was used as the selected sample for NF calculations.

Signals were adjusted using the formula (Calculated PI)/(Calculated NF). SimpleChIP® Human RPL30 Exon 3 Primers (Cell Signaling Technology) were used in conjunction with the control antibodies to confirm the success of the performed CUT&RUN assay.

2.11. Analysis of miRNA target genes

For the prediction of canonical target genes of differentially expressed miRNAs, miRWalk was used [24], as it combines the database of experimentally validated miRNA targets (DIANA-TarBase) and tools for the prediction of miRNA targets (TargetScan and miRDB). Only target genes that were validated or predicted with both tools were used for further analysis. Target genes of downregulated miRNAs were then intersected with differentially expressed genes between the MES-OV CBP and MES-OV cell lines [16]. Only upregulated genes (FC $>$ 2, P $<$ 0.05) passed the negative correlation filter (in regards to downregulated miRNAs). The expression of selected target genes was measured by RT-qPCR as previously described [16]. *GAPDH* served as an internal control. The primer sequences are listed in Table S1.

2.12. Signaling pathway analysis

A pathway analysis of differentially expressed genes (DEGs) of three miRNAs of interest (miR-17, miR-103a, miR-107) was performed to provide insight into possible mechanisms by which these miRNAs alter the acquired resistance to CBP and/or metastatic potential of MES-OV CBP cells. The analysis was performed using a Database for Annotation, Visualization and Integrated Discovery (DAVID) [19,25] linked to the KEGG. The KEGG pathway enrichment analysis was performed to identify biological processes involving predicted target genes. P $<$ 0.05 and a gene count of at least 3 were the cut-off criteria.

2.13. Transient transfection with miRNA mimics and inhibitor

DharmaFECT transfection reagent was combined either with miRIDIAN microRNA Mimic miR-17–5p, 103a–3p, 107 or scrambled negative control, or with miRIDIAN miRNA Hairpin Inhibitor miR-103a–3p or negative control (Horizon Discovery, a PerkinElmer Company, UK) at a final concentration of 25 nM, and incubated in OPTI-MEM (GIBCO Life Technologies) for 20 min prior to addition to the MES-OV cell pair. Cells were incubated at 37 °C for 48 h, then seeded for the cell viability assay, collected for RNA isolation and seeded for cell migration and invasion assays.

2.14. Analysis of the prognostic and predictive values of genes

The prognostic value of selected miRNAs was analyzed using KM Plotter's miRpower tool [26]. Curated datasets from Gene Expression Omnibus (GEO), European Genome-phenome Archive (EGA), and the Cancer Genome Atlas (TCGA) were used for the overall survival (OS) analysis. Only OC patients were selected and split automatically by the best cut-off value. Data were presented as *Kaplan Meier* plots, with a hazard ratio (HR) and log-rank p-values. Expressions of selected miRNAs in different stages of ovarian serous cystadenocarcinoma (I, II, III, IV) were explored by the TCGA miRNA tool of the UALCAN data analysis portal [27]. Results were presented on box-whiskers plots, along with P values calculated by Student's t-test. The predictive value of selected miRNAs was explored by Receiver Operating Characteristic (ROC) Plotter tool [28] on ovarian serous cystadenocarcinoma samples from patients that received carboplatin therapy. Value of miRNAs to predict treatment response (responders vs non-responders after completing the therapy and after median follow-up time (33 months)) was evaluated by comparing expressions of miRNAs in two groups (non-responder vs responder), generating the *ROC* plots and calculating the AUC values. Results were presented as *box and whiskers* plots with Mann-Whitney P values and ROC plots with AUC and *ROC* P values. Results with a P value $<$ 0.05 were considered significant.

2.15. Statistical analysis

RT-qPCR data were analyzed by unpaired Student's t-test and expressed as the mean ± standard error of the mean. Experiments were performed in triplicate and repeated at least twice. Survival assays were analyzed by two-way ANOVA with Bonferroni's post hoc tests, while wound healing and invasion assays were analyzed by one-way ANOVA with Dunnet's post hoc tests. Analyses were performed in GraphPad Prism 9. These experiments were performed in quadruplicate and repeated at least twice, if not indicated differently.

3. Results

3.1. Cells with acquired, drug-induced mesenchymal-like phenotype display different miRNA expression profile and show sensitivity towards epigenetic modulators

MiRNA microarray covering 752 human miRNAs was performed on two biological replicas of sensitive MES-OV and CBP-resistant MES-OV CBP cell lines established previously [16]. This well-characterized, solid *in vitro* and *in vivo* model of OC [29,30] has been shown useful for gene expression profiling [16]. Based on the fold change (FC $>$ 1.25) and minimal variance between replicas, 29 upregulated and 48 downregulated miRNAs were detected in MES-OV CBP compared to the parental MES-OV cell line (Fig. 1A; listed in Table S2). Differentially expressed miRNAs were distributed on almost all chromosomes, and several clusters with more than one member were identified among downregulated miRNAs (Fig. 1A).

One of the molecular mechanisms for drug resistance is epigenetic modulation. In clinical practice, a combination of epigenetic modulators and drugs has been considered as a possible future therapy approach [31]. Interestingly, while treatment with 5-aza or TSA separately did not impact the viability of MES-OV CBP cells, a combination of both inhibitors significantly sensitized cells to drug treatment (Fig. 1B). Due to the known mesenchymal-like phenotype of the MES-OV CBP cell line [16], the impact of 5-aza and TSA treatment was investigated regarding cell migration and invasion. Despite the repeated tendency of reduction of migratory capacity of MES-OV CBP cells upon combination treatment with two epigenetic inhibitors, the differences were not statistically significant (Fig. 1C). However, the invasion capacity of the MES-OV CBP cell line was reduced to the capacity of the untreated parental MES-OV cell line (Fig. 1D). Obtained data implied that changes in DNA methylation and histone deacetylation probably affected the activity of different promoters in MES-OV CBP cell line, resulting in gene and miRNA repression and increased drug resistance and invasiveness.

3.2. Multilevel selection with epigenetic modulators and two other OC cell pairs identifies triple miRNA-signature for OC cell lines with acquired mesenchymal-like phenotype

Based on the known fact that DNA methylation and histone deacetylation are linked to gene silencing [32], we focused on the downregulated miRNAs and hypothesized that their expression could be regulated epigenetically [33–35]. The list of downregulated miRNAs was subjected to a comprehensive literature search in the context of drug resistance and epithelial-mesenchymal transition. We noticed that some of the miRNAs downregulated in the MES-OV CBP cell line are grouped in clusters (Table S3). Since it is accepted that clustered miRNAs are regulated in the same manner due to the shared promoter [36,37], we further narrowed down the list in a way that only one member of the cluster was chosen as a representative for validation. The members of miR-200 family are the subject of investigation in another study and therefore not included here. The members of let-7 family were not followed further due to their well-known role in cancer stemness, drug

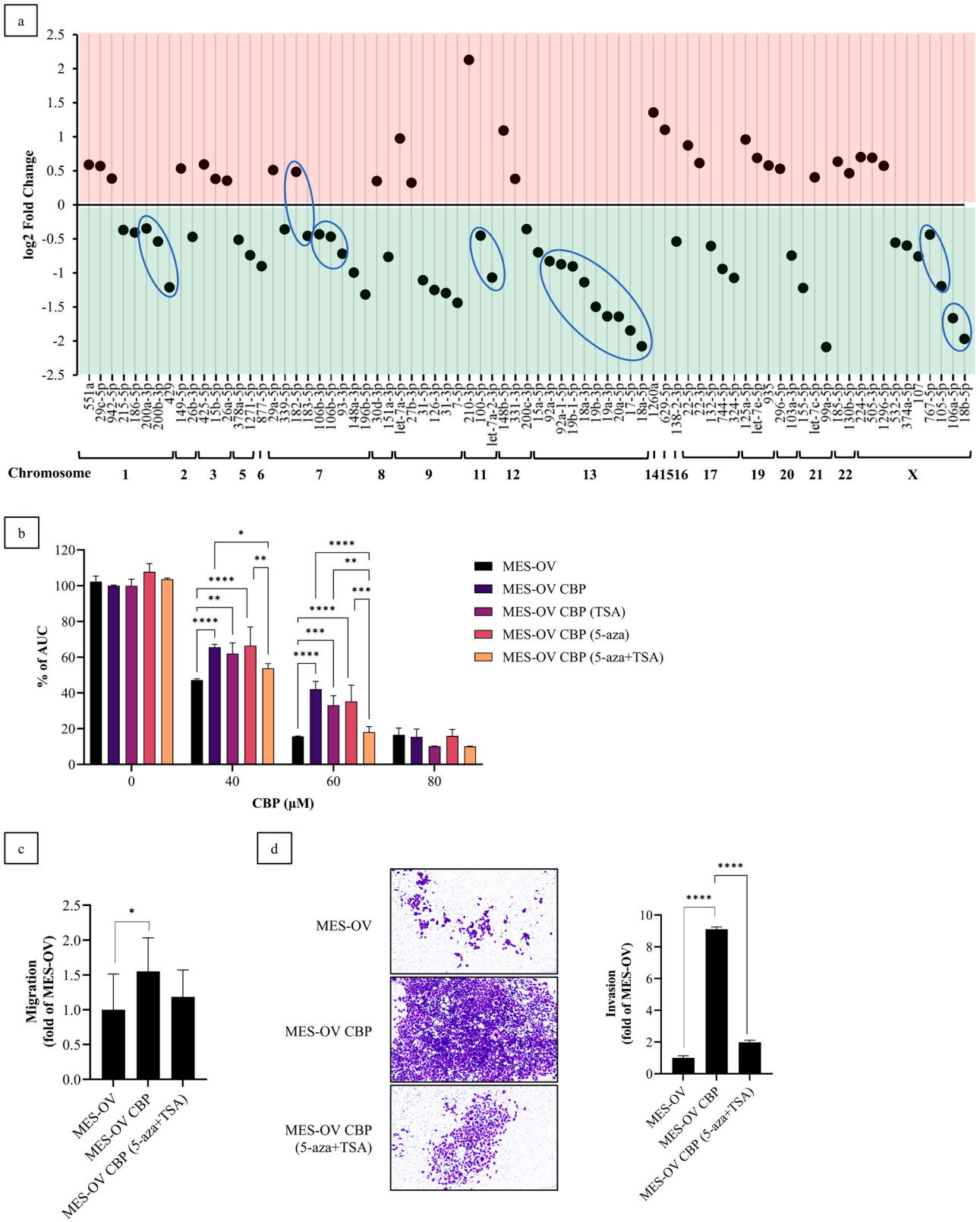

Fig. 1. MiRNA expression pattern of MES-OV cell model and impact of epigenetic modulators on drug response and metastatic potential of MES-OV CBP cells (A) Upregulated (red shade) and downregulated (green shade) miRNAs are shown. Expression change between MES-OV CBP and MES-OV cells is presented as $\log_2$ Fold Change. The location of deregulated miRNAs on chromosomes is indicated. Deregulated miRNAs that are part of the same cluster are circled. (B) Twenty-four h after seeding, cells were co-treated with 1 μM 5-aza or 33.3 nM TSA or their combination, and different concentrations of CBP for 72 h (media with freshly added compounds was changed every 24 h). Untreated MES-OV CBP control was set as 100% to calculate % of AUC. (C) Twenty-four h after seeding, cells were treated with 5-aza and TSA. The day after, they were seeded into a 24-well plate and their migration was measured by wound healing assay. Results were presented as a fold of migrated cells after 6 h compared to MES-OV cells. The average values of three independent experiments were shown. (D) Total areas covered by invaded cells (AUC) were measured and expressed as folds of MES-OV. A representative experiment out of three is shown. (*, $P < 0.05$; **, $P < 0.01$; ***, $P < 0.001$; ****, $P < 0.0001$).

resistance and in reversing drug-induced EMT [38,39]. In total, 14 microarray-extracted downregulated miRNAs were validated by RT-qPCR and nine were confirmed to be significantly downregulated in the MES-OV CBP compared to the MES-OV cell line (Fig. 2A). Furthermore, the expression of seven miRNAs was restored in MES-OV CBP cells after the treatment with inhibitors, implying the possibility of their epigenetic regulation by DNA methylation and histone deacetylation (Fig. 2B).

To validate our findings on a more general level and to avoid focusing on a potential cell line-specific effect, we explored the expression of selected seven miRNAs in two other AMP epithelial OC cell lines; SK-OV-3 CBP (non-serous OC) and OVCAR-3 CBP (high-grade serous OC) and their appropriate parental cell lines, SK-OV-3 and OVCAR-3. From seven selected miRNAs, only three had a similar pattern of expression as the one seen in the MES-OV cell pair: miR-17–5p, miR-103a–3p and miR-107 (Fig. 2C). This indicated that these three miRNAs could be considered and analyzed as possible miRNA-signature markers for OC cell lines with acquired, drug-induced mesenchymal-like phenotype.

Based on previously published [12,16], as well as unpublished data, and gained experience regarding possible functionality/non-functionality of selected candidate molecules, we decided first to forecast their possible involvement in drug resistance and drug-induced EMT before performing functional tests.

3.3. Selected miRNAs modulate several signaling pathways in cancer

Our next interest was to investigate the involvement of three selected miRNAs in signaling pathways via predicted target genes, with a focus on pathways involved in drug resistance and drug-induced mesenchymal-like phenotype. To avoid a non-specific approach and to identify miRNA target genes relevant to the cell model of interest, we used data from previously performed mRNA assay in which the screening of over 21,000 genes of MES-OV and MES-OV CBP cell lines was executed [16]. The intersection of differentially expressed genes (DEG; fold change >2, $p < 0.05$) and miRNA target genes, obtained by miRWalk [24] for miR-17–5p, miR-103a–3p and miR-107 was performed. Additionally, we concentrated only on upregulated target genes, as negative correlation corresponds with the widely accepted mechanism of action of miRNAs [40] (Fig. 3A). The Venn diagram shows unique and overlapping target DEGs of the three selected miRNAs (Fig. 3B right), all of them upregulated in MES-OV CBP more than two-fold compared to the MES-OV cell line (Fig. 3B left). Two genes, PIK3R1 and ABL2 were identified as shared targets of three miRNAs. The obtained target DEGs of miR-17–5p, miR-103a–3p and miR-107 were then pooled together and further analyzed using the database for annotation, visualization and integrated discovery (DAVID) [41,42] to identify their enrichment in biological pathways. KEGG pathway analysis revealed the enrichment in several cancer-related signaling pathways, the most significant of which were Ras and ErbB signaling pathways (Fig. 3C; Table S4). Except for *PIK3R1* and *ABL2,* the expression of *PAK3,* a unique miR-103a–3p

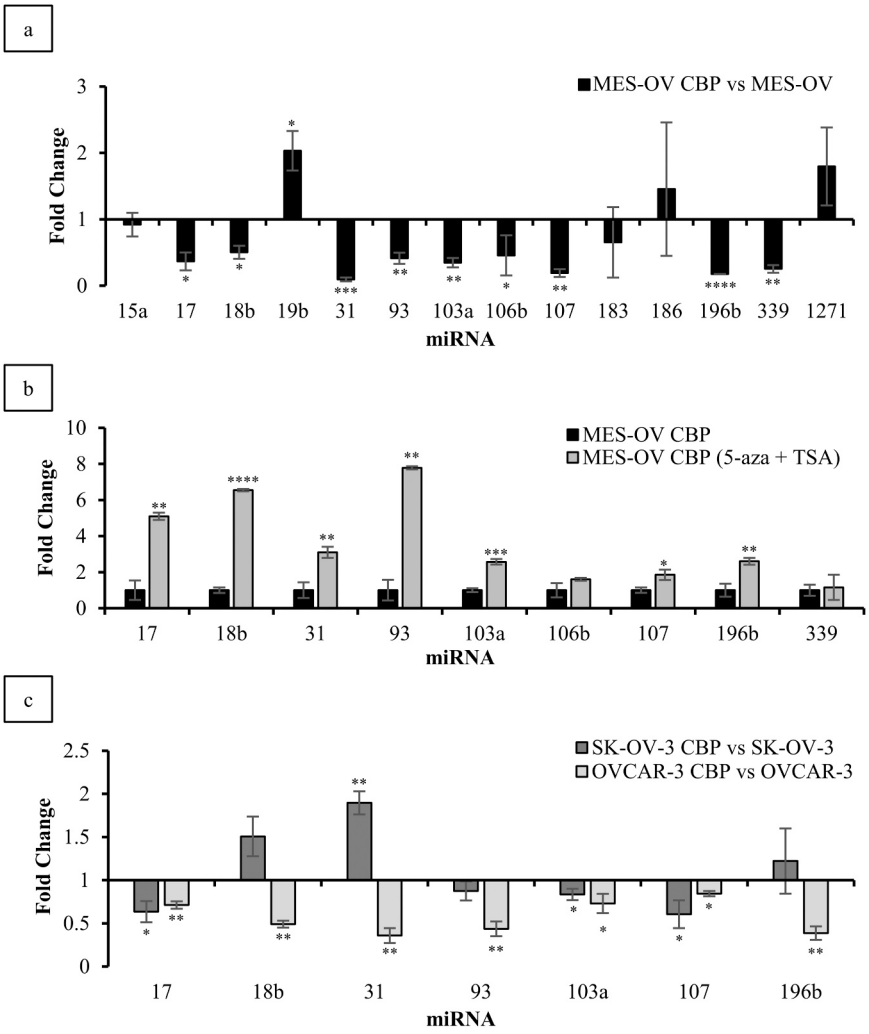

Fig. 2. Selection of downregulated miRNAs in MES-OV CBP cells by RT-qPCR validation, epigenetic modulators and other CBP-induced AMP cell lines (A) Constitutive expression of selected miRNAs, (B) the expression of selected miRNAs in MES-OV CBP cells after 72 h of treatment with 1 μM 5-aza and 33.3 nM TSA and (C) the constitutive expression of selected miRNAs in two other CBP-resistant ovarian cancer cell lines was determined by RT-qPCR. *RNU6* was used as an internal loading control. Fold change of expression was calculated between resistant compared with parental cell line (A and C) or treated compared to untreated cell line (B). The parental (A and C) or untreated (B) line was set as 1. (*, $P < 0.05$; **, $P < 0.01$; ***, $P < 0.001$; ****, $P < 0.0001$).

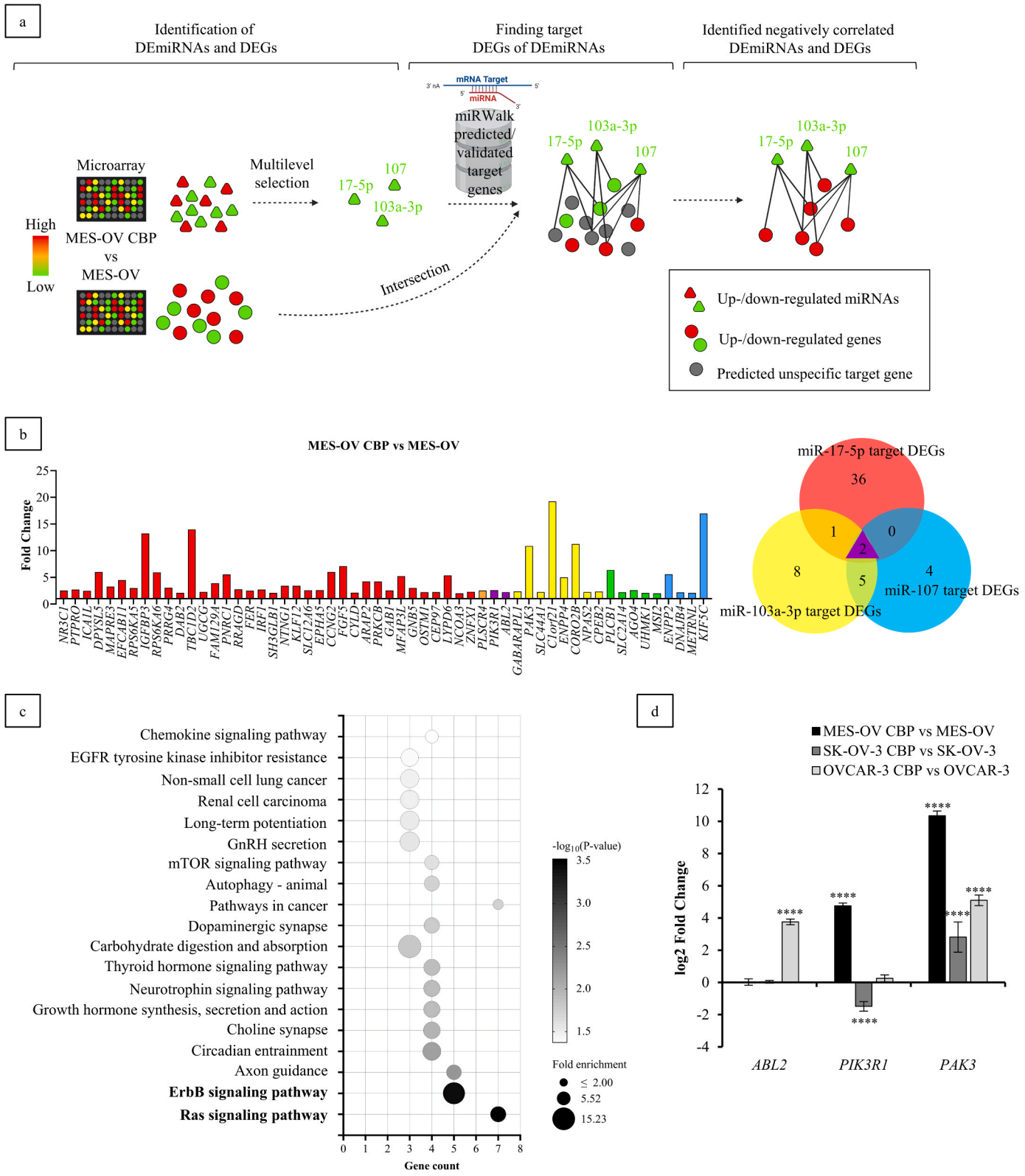

Fig. 3. Pathway analysis of three-miRNA signature target DEGs (A) Deregulated genes (Fold change >2, $P < 0.05$) obtained by analysis of gene expression between MES-OV and MES-OV CBP cell lines by microarray [16] and target genes (miRWalk) of microarray-derived deregulated miRNAs were intersected. Target genes passed the filter only if validated or predicted in TargetScan and miRDB. Upregulated target genes of three miRNAs of interest were identified and used for further analysis. The illustration is created in BioRender (BioRender.com). (B) The Venn diagram shows unique (red, yellow and blue) and overlapping (orange, green and purple) target DEGs of the three selected miRNAs (right), all of them upregulated in MES-OV CBP more than two-fold compared to the MES-OV cell line (left). (C) Target DEGs were classified into pathways using DAVID (KEGG). $P < 0.05$ and a gene count of at least 3 were the cut-off criteria. (D) The expression of three target DEGs, *ABL2*, *PIK3R1* and *PAK3* was checked by RT-qPCR 48 h after cell seeding, using *GAPDH* as an internal loading control. Expression change between CBP-resistant and parental cells is presented as $\log_2$ Fold Change. The parental line was set as 0. (*, $P < 0.05$; **, $P < 0.01$; ***, $P < 0.001$; ****, $P < 0.0001$).

predicted downstream target that is also involved in the Ras and ErbB signaling pathways (Table S4), was checked. Expression analysis of selected genes resulted in a pattern pointing towards miR-103a–3p as an interesting candidate due to increased expression of its unique target *PAK3* in three different CBP-induced AMP OC cell lines compared with their appropriate parental cells (Fig. 3D).

3.4. Exogenous modulation of miR-103a–3p expression affects the invasive capacity of both CBP-resistant and parental cells

Since the selection of three miRNAs was supported by the results of signaling pathways analysis, functional overexpression tests were performed. The transfection itself did not impact cell growth and/or cell viability compared to non-transfected cells (data not shown). It is interesting that despite the use of the same mimic concentration for all miRNAs transfections, the impact of mi(107) on the expression of miR-107 was much stronger than the other two mimic sequences on corresponding miRNAs (Fig. 4A). Although the intersection of DEGs and miR-17–5p, miR-103a–3p and miR-107 target genes did not directly result in signaling pathways involved in drug resistance, suggesting that these miRNAs do not have a role in this process, possible effect of the overexpression of three downregulated miRNAs on CBP-induced stress was also explored since the acquired downregulation was carboplatin-induced. Surprisingly, transfection of MES-OV CBP cells with mi(17), mi(103a), and mi(107) resulted in decreased sensitivity to CBP treatment, making cells 1.5, 1.3 or 1.4 fold (comparison of IC_{50} of CBP-resistant cells transfected with mi(17), mi(103a) or mi(107)/IC_{50} of CBP-resistant cells transfected with mi(-)) less sensitive to CBP compared with the cells transfected with non-targeting control (Fig. S2A). Migration assay confirmed MES-OV CBP cell line transfected with non-target control is more migratory than MES-OV control. Additionally, only transfection with mi(103a) decreased the migratory potential of MES-OV CBP compared with MES-OV CBP control cells (Fig. 4B). Further, MES-OV CBP showed a strong invasive capacity

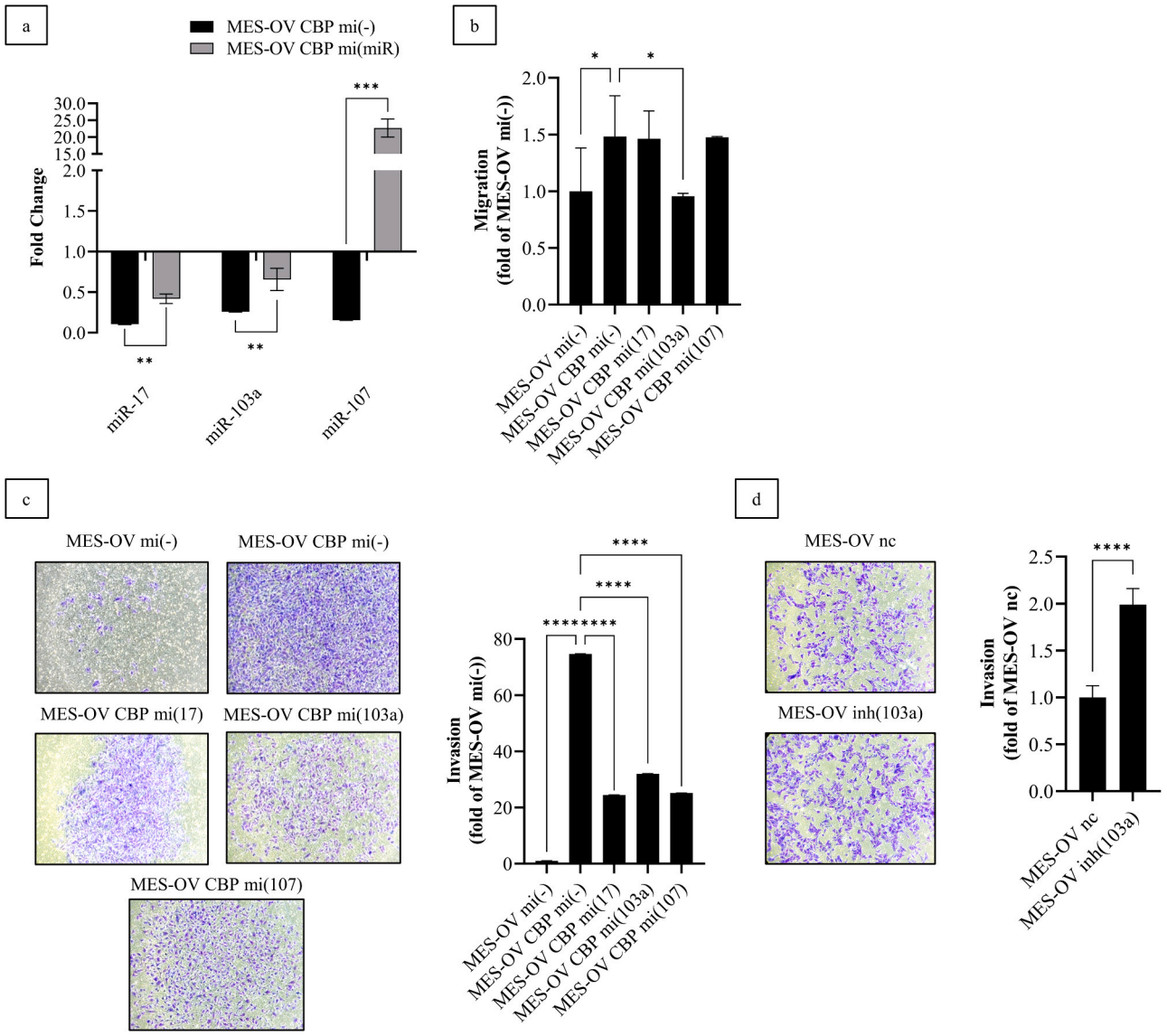

Fig. 4. Functional analysis of selected miRNAs in MES-OV CBP cells (A) Forty-eight h after transfection with mi(-), mi(17), mi(103a) and mi(107) the expression of miR-17–5p (miR-17), miR-103a–3p (miR-103a) and miR-107 (miR-107) was measured using *RNU6* as an internal loading control. The MES-OV mi(-) was set as 1. (B) Transfected cells were re-seeded and their migration was measured. Results are presented as a fold of migrated cells after 6 h compared to MES-OV mi(-) cells. The average values of three independent experiments are shown. (C) Transfected cells were re-seeded for the invasion assay. Total areas covered by invaded cells (AUC) were measured and expressed as folds of MES-OV mi(-). Representative experiment out of three is shown. (D) MES-OV cells transfected with negative control (nc) and miR-103a–3p inhibitor (inh(103a)) cells were seeded for invasion assay as described under (C). (*, $P < 0.05$; **, $P < 0.01$; ***, $P < 0.001$; ****, $P < 0.0001$).

compared with MES-OV control cells, while all three miRNAs impaired the invasion of MES-OV CBP cells (Fig. 4C). Based on the impact on both migration and invasion, we further focused on miR-103a–3p. Inhibition of miR-103a–3p (inh(103a)) potentiated the invasion of MES-OV cells compared with MES-OV (nc) (Fig. 4D). Interestingly, inhibition did not impact the sensitivity of MES-OV cells toward CBP (Fig. S2B), supporting the signaling pathway analysis data prediction showing that miR-103a–3p probably does not have a role in MES-OV cell pair response to CBP. In order to explore if the observed role of miR-103a–3p is cell type dependent or if it could be a feature of HGSOC cells with CBP-induced AMP, all experiments were repeated on the OVCAR-3 cell pair. Not only that obtained data were similar to the response of the MES-OV cell pair, they were even more pronounced, probably due to the more considerable difference in the EMT character and metastatic potential between parental OVCAR-3 and resistant OVCAR-3 CBP cell line (Fig. S1 and S3).

3.5. The miR-103–3p promoter in CBP resistant cells is characterized by higher methylation and lower enrichment in H3K27ac mark

Methylation status of miR-17–5p, miR-103a–3p and miR-107 promoters was checked to explore the hypothesis about the possible epigenetic regulation of their expression. Interestingly, unmethylated (U) DNA was observed in the MES-OV and MES-OV CBP cell lines for all three miRNA promoter CGIs, but methylated DNA (M) only for miR-103a–3p and miR-107 (Fig. 5A). The CGI encompassing the miR-17–5p host gene (*MIR17HG*) transcription start site and its first exon is > 1000 bp larger than CGIs surrounding the promoters of miR-103a–3p and miR-107, so two MSP assays for miR-17–5p were designed for better CGI coverage (Fig. S4). The specific PCR products for the methylated miR-17–5p promoter fragments were not detected in either assay, while the same reactions with control methylated bisulfite converted EpiTect DNA resulted in the amplification of expected specific bands (data not shown). Further, miR-103a–3p promoter methylation was more prominent in MES-OV CBP cells compared with the parental cell line and it reverted to the methylation level of parental cells promoter upon treatment with 5-aza and TSA. This implied miR-103a–3p could be epigenetically silenced at the constitutive level in the MES-OV CBP cell line. The observed downregulation of miR-17–5p and miR-107 in the MES-OV CBP cell line compared with MES-OV cells seemed to be independent of the promoter methylation status (Fig. 5A). Higher methylation of the miR-103a–3p promoter was also confirmed for the OVCAR-3 CBP cells compared with the parental OVCAR-3 (Fig. S5A).

Additionally, the acetylation of the lysine residue at N-terminal position 27 of the histone H3 protein (H3K27ac) of the promoter, as a known marker of active promoters and enhancers [43,44], was also examined. Obtained data showed that the H3K27ac signal is weaker at the constitutive level in MES-OV CBP cells compared with parental MES-OV cells for all three examined miRNA promoter regions and elevated after the treatment with epigenetic inhibitors (Fig. 5B). Similar data were obtained for OVCAR-3 CBP cells (Fig. S5B).

3.6. Selected miRNAs have a prognostic value in a group of OC patients with enrichment in mesenchymal stem cells (MSC)

The association between chemoresistance and the acquisition of

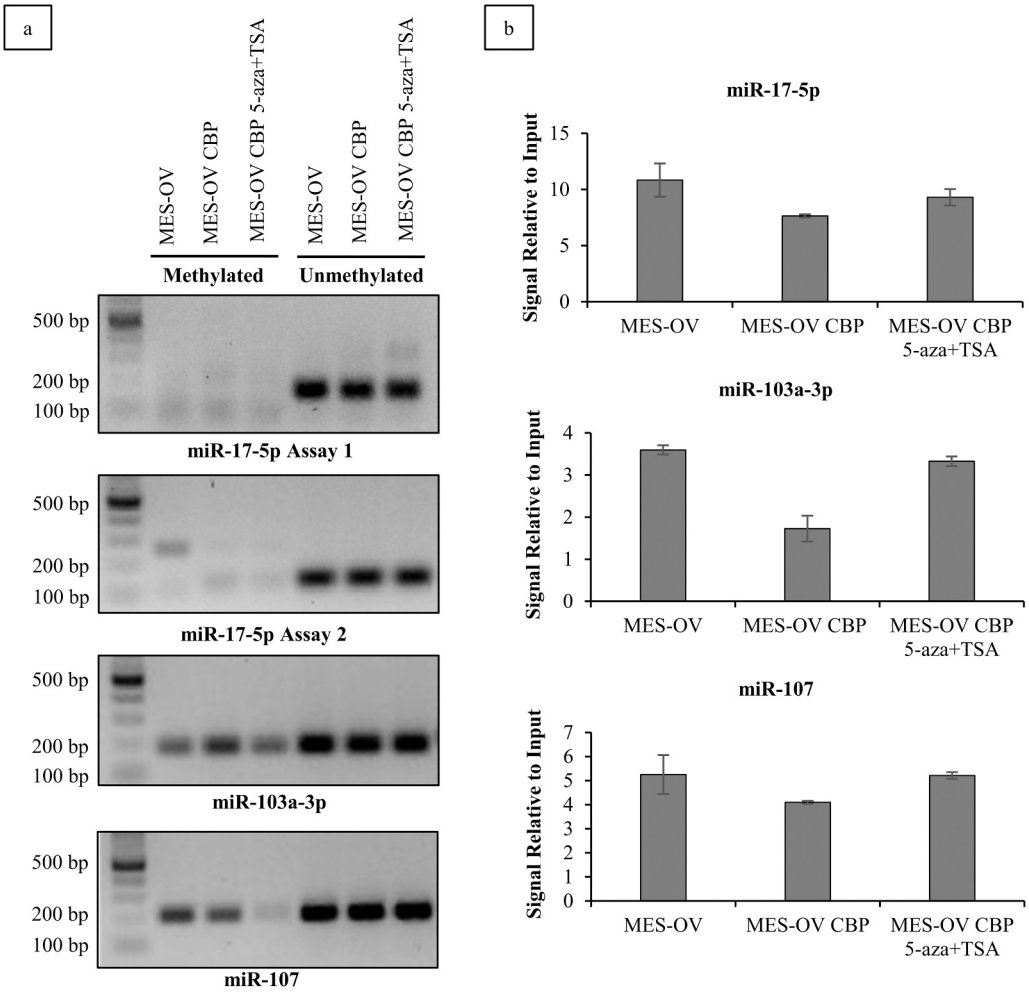

Fig. 5. Epigenetic analysis of selected miRNAs in MES-OV CBP cells (A) The methylation status of conserved CpG islands (CGIs) in the promoter sequences was analyzed by specific amplification of methylated (M) and unmethylated (U) DNA fragments, and (B) the enrichment of the H3K27ac activating mark in promoters was assessed by CUT&RUN experiments. Individual qPCR reactions performed in triplicates are presented as mean ± SD and are representative of two independent experiments.

mesenchymal-like and ovarian cancer stem cell-like phenotypes has been demonstrated previously [45]. The expression of several genes associated with stemness indicates stem-like phenotype of MES-OV CBP compared to the parental cells (Table S5). Therefore, the further goal was to explore the possible application of miR-17–5p, miR-103a–3p and miR-107 as pharmacological biomarkers for prediction of patients' survival and response to therapeutic intervention. Prognostic values of selected miRNAs on two groups of OC patients, „All" and „MSC: enriched" (samples with high content of mesenchymal stem cells), were examined by selecting miRNAs and defining integrated restriction filters integrated miRpower tool [26]. Expression of miR-17–5p did not have any predictive value in two observed groups of OC patients. On the other hand, OS of OC patients with high miR-103a–3p expression was just slightly higher compared to all OC patients with low expression, while the effect was more significant in the group of OC patients with enriched MSC. High expression of miR-107 was significantly better at forecasting the OC patients' OS in both observed groups (Fig. 6A). Obtained data show that based on correlations between gene expression and overall survival, miR-103a–3p and miR-107 have a prognostic value for OC (Fig. 6A), especially in the case of patient samples with an observed enrichment in MSC, while miR-17–5p does not. It is interesting to emphasize that these two miRNAs could be valuable prognostic markers for other types of tumors as well (Table S6-S8). Analysis using UALCAN revealed differences in miR-103a–3p and miR-107 expressions between different stages of ovarian cancer (Fig. 6B). Based on the fact that later stages of OC are often accompanied by higher metastatic potential and drug resistance and result in treatment failure, predictive value of three miRNAs was also explored using the ROC Plotter (Fig. S6). When analyzing the response to therapy immediately after its completion (Treatment response), the results confirmed that miR-107 expression is downregulated in the group of patients that do not respond to CBP. The same but non-significant effect was observed in the case of miR-103a–3p (Fig. S6). Consequently, only these two had increased AUC values (with miR-107 having the most prominent results), suggesting their potential value in predicting the response to CBP therapy. However, when the response to therapy was analyzed after 33 months, miR-17–5p and miR-103a–3p were significantly downregulated in the non-responders group and had increased AUC values (Fig. S6). To sum it up, results suggest miR-107 could predict early response to CBP therapy, while miR-17–5p and miR-103a–3p could predict the long-term response.

4. Discussion

Ovarian cancer is the seventh most common cancer among women worldwide, having the highest fatality-to-case ratio of all gynecological malignancies [3,13]. Expression profiling, such as microarray and RNA-seq, has been extensively used *in vitro* and *ex vivo* to gain insight into gene dysregulation, which could lead to improved therapy options [46]. Here, the microarray profiling of miRNAs in the stable, well-characterized, drug-induced AMP MES-OV CBP [16] versus parental MES-OV cell line led to the identification of 29 upregulated and 48 downregulated miRNAs. DNA methylation and histone deacetylation

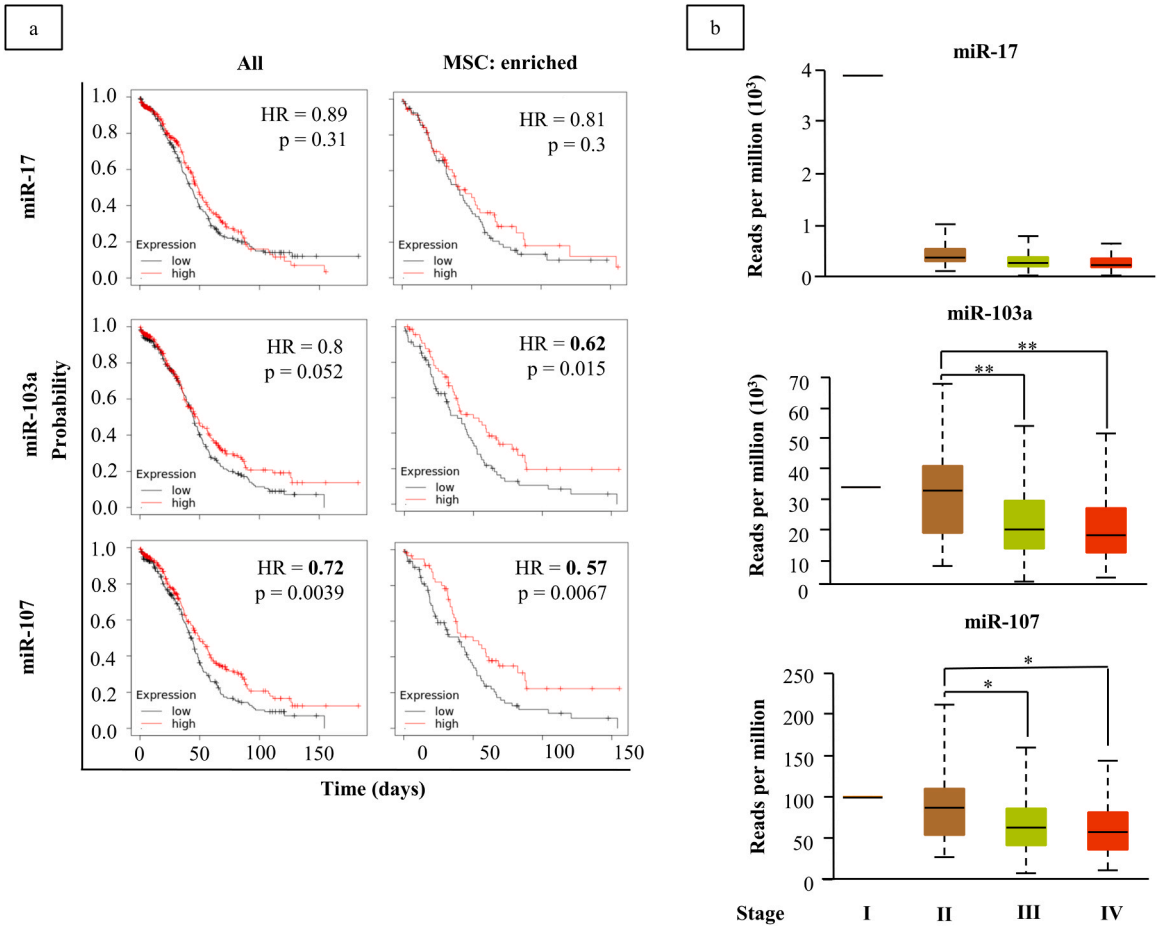

Fig. 6. Analysis of prognostic values of miR-17–5p, miR-103a–3p and miR-107 (A) Prognostic values of miR-17–5p, miR-103a–3p and miR-107 were analyzed on cohorts of all patients with ovarian serous cystadenocarcinoma (n = 485) and the specific subset with enriched mesenchymal stem cells (MSC, n = 151). Overall survival (OS) was analyzed and presented as *Kaplan Meier* plots, along with HR and log-rank p-values. (B) Expressions of miR-17, miR-103a–3p and miR-107 were explored in 473 TCGA samples from patients with ovarian serous cystadenocarcinoma. Results were plotted as *box-whiskers* plots of mean reads per million versus cancer stages. Statistical significance was calculated by the student's t-test. (*, P < 0.05; **, P < 0.01; ***, P < 0.001; ****, P < 0.0001).

regulate different miRNAs and impact the development of therapy resistance [32] and cancer metastasis [47]. The importance of these epigenetic modifications in response to the therapy is emphasized with the extensive research focused on the potential use of 5-aza and TSA for reversing epigenetically repressed genes as an addition to regular therapy [31]. Our results comply with this, as co-treatment of MES-OV CBP cells with the combination of these inhibitors, rather than individual treatment, led to their sensitization to the CBP. Additionally, even though combinatorial treatment with inhibitors did not significantly affect the migration of MES-OV CBP cells, it impaired their invasion capability.

We focused on downregulated miRNAs, proposing that this downregulation could be due to epigenetic repression. From 14 selected, nine miRNAs passed the validation by RT-qPCR and were investigated further. To avoid the detection of cell-specific changes, we used the other two epithelial OC cell lines established in our laboratory, SK-OV-3 CBP and OVCAR-3 CBP [16]. While these cell models share some characteristics with MES-OV CBP (resistance to CBP and mesenchymal-like phenotype), they differ in their sensitivity to other DNA-damaging or tubulin-binding agents, suggesting differences in gene expression pattern and cell stress response (unpublished data). Also, the SK-OV-3 cell pair differs in their origin [48]. This fact makes finding common changes in miRNAs across all three cell models more significant. Only miR-17–5p, miR-103a–3p and miR-107 shared a similar expression pattern in all analyzed OC cell models, implying these miRNAs could potentially be interesting for a broader spectrum of epithelial OC patients (HGSOC and non-serous OC).

In order to understand the possible roles of miR-17–5p, miR-103a–3p and miR-107 in resistant AMP OC cells, miRNA target prediction and pathway analysis were performed. To avoid the likelihood of false prediction [49], more databases for target prediction and overlap of their results were used. We selected the miRWalk database as it combines a database of experimentally validated miRNA targets (DIANA-TarBase) and tools for the prediction of miRNA targets (TargetScan and miRDB). However, this still left us with a large number of target genes to explore. It is very challenging to determine the primary functions of specific miRNAs, as they are tissue-related. This is visible from a high number of conflicting roles of the same miRNA in different tissues [49]. Therefore, transcriptomic data from the same experimental model is necessary, as miRNA profiling coupled with mRNA profiling enables the avoidance of false positive target gene identification and focuses the research on specific targets. Following this, we intersected miRWalk-obtained target genes of three miRNAs of interest with differentially expressed genes derived from the mRNA microarray of the MES-OV cell pair [16]. This left us with 56 target DEGs, some shared between the three selected miRNAs and some unique, that were pooled and used for the pathway analysis. We used DAVID and its connection to the KEGG database to cluster the list of target DEGs into cellular pathways. Analysis showed that ErbB and Ras signaling pathways, known to be related to invasion and migration [50,51], are the most affected by miR-17–5p, miR-103a–3p and miR-107, with *PIK3R1* and *ABL2*, only shared targets of all three miRNAs, contributing to these two pathways. Unique miR-103a–3p target *PAK3,* with high degree of expression change, was also recognized as the participant of both signaling pathways. Notably, ErbB signaling is linked to the initial steps of epithelial-mesenchymal transition (EMT) as integrins, focal adhesion kinase and Rho GTPases, important regulators in mesenchymal-type migration, may be influenced by this pathway [15]. Downstream functional effects of the Ras signaling pathway, also connected to mTOR signaling, influence apoptosis, cell metabolism, cell motility and migration [31]. Further exploration is needed to identify the functionality of signaling pathways as well as *PIK3R1*, *ABL2* and *PAK3* as possible downstream targets of selected miRNAs, and their potential role in drug-induced AMP.

Indeed, our data showed that miR-17–5p, miR-103a–3p and miR-107 are involved in the metastatic potential of MES-OV CBP cells, also corresponding to the literature data. Notably, miR-17–5p, depending on the cellular contexts, can act as an oncogene and tumor suppressor gene [52]. It promotes the invasion and migration of colorectal cancer [37]. On the other hand, miR-17–5p inhibits OC peritoneal metastasis of SK-OV-3 xenografts [53]. We have to emphasize that regarding miR-17–5p, which is a part of miR-17/92 cluster, there is a possibility that other members of the cluster, such as miR-18a, miR-19a, miR-20a, miR-19b-1 and miR-92a-1 [54], could have an impact on MES-OV CBP impassivity by targeting different genes. High levels of miR-103a–3p were associated with a better prognosis for patients with non-small cell lung cancer (NSCLC). Its possible role in modulating the malignant behavior and stemness of cancer cells makes it a potential therapeutic target for the management of NSCLC [45]. The knockdown of miR-103a–3p expression inhibited tumor oral squamous cell carcinomas growth and enhanced the activity of cisplatin in a xenograft animal model [55]. MiR-103a–3p mimics promoted the proliferation and invasion of NSCLC cells through the Akt pathway by targeting PTEN, suggesting miR-103a–3p as a novel therapeutic target for NSCLC [56]. However, there is a lack of data about the role of miR-103a–3p in the drug resistance and drug-induced metastatic potential of OC cells, especially regarding CBP. On the subject of miR-107, published data describe this miRNA as a tumor suppressor. Overexpression of miR-107 reduced melanoma cell proliferation, migration and invasion [57] and metastasis of human NSCLC [58], having pleiotropic functions in cancer networks [59]. Also, ectopic expression of miR-107 suppressed OC SKOV3 cell proliferation and induced cell cycle arrest and was associated with the downregulation of cyclin E1 expression [60]. Regarding our data, we showed for the first time the importance of miR-103a–3p, miR-17–5p and miR-107 in invasion capacity and miR-103a–3p in migratory capacity of OC cell lines with acquired resistance to carboplatin. Although we expected an increase in the sensitivity of MES-OV CBP cells to CBP upon transfection with appropriate mimic sequences, the opposite was obtained, as the MES-OV CBP cell line became less sensitive to CBP compared to the control. In our previous work, we showed that increased expression of miRNA-200 family members in paclitaxel-resistant and CBP cross-resistant OVCAR-3 TP GFP cells also surprisingly decreased sensitivity to CBP despite their downregulation at the constitutive level [12]. At the moment, we cannot explain this phenomenon. There is a possibility that some kind of miRNAs micromanagement exists [61]. We can exclude the possibility that the supraphysiological levels of mature miRNAs led to non-specific changes in gene expression [62] since the MES-OV CBP cells transfected with a broad range of mimic concentrations always showed the same effect, decreased sensitivity to CBP compared to the negative control (data not shown). Building on this and focusing on epigenetically regulated miR-103a–3p, we showed that transfection of parental MES-OV cells with miR-103a–3p inhibitor did not change the sensitivity of cells to CBP, however it enhanced the invasion of MES-OV cells, indicating possible role of miR-103a–3p in the drug-induced metastatic potential but excluding its role in the response of cells to cytostatic.

Finally, the fact that a combination of epigenetic modulators restored miR-17–5p, miR-103a–3p and miR-107 expression made us wonder whether this is a consequence of upstream modulations or whether there is a possibility that all three promoters are epigenetically modulated at the constitutive level as a result of acquired AMP. The MSP promoter analysis demonstrated the epigenetic silencing of miR-103a–3p via promoter CGI methylation in MES-OV CBP and OVCAR-3 CBP cells in comparison with their parental cell line. When taken together with the scratch assay results upon 5-aza and TSA treatment, these results imply that methylation-associated silencing of miR-103a–3p promotes invasiveness in our AMP OC cell models. Interestingly, at the constitutive level in MES-OV and OVCAR-3 cell models, miR-103a–3p and miR-107 promoters displayed methylated and unmethylated forms, while miR-17–5p promoter displayed only unmethylated form. Moreover, the methylation status of miR-103a–3p and miR-107 promoters could be epigenetically modulated. However, only downregulation of miR-103a–3p, detected at a constitutive level in AMP

cell lines, seems epigenetically regulated. There are no visible differences in promoters' methylation status in the MES-OV and OVCAR-3 cell pair for miR-17–5p and miR-107 promoters. Furthermore, the enrichment for H3K27ac, which is associated with the activation of transcription and therefore defined as an active chromatin mark [63], is lower in MES-OV CBP cells compared with MES-OV cells for analyzed promoter regions. This data correlates well with the expression of three miRNAs of interest. It is known that histone deacetylase inhibitor SAHA epigenetically regulates miR-17–92 cluster in human hepatoma HepG2 and H7402 cell lines [64]. Herein we demonstrated for the first time the tendency of CBP to induce differences in acetylation of the miR-17–5p, miR-107 and miR-103a–3p promoters in drug-resistant OC cells compared with parental cell lines at the constitutive level. However, it is known that transcription regulation of miRNA expression can be regulated by different transcription factors, or post-transcriptionally, by changes in miRNA processing [65], not only epigenetically. The fact that both methylated (miR-107 and miR-103a–3p) and unmethylated forms of analyzed fragments are present, as well as differences in histone acetylation, implies these promoters can be modulated by epigenetic inhibitors (corresponding to the results presented on Fig. 2B), which is interesting in the context of possible combination of chemotherapy and treatment with epigenetic modifiers [25].

Furthermore, since data obtained for the MES-OV cell pair were confirmed on the OVCAR-3 cell pair, it seems that the above-described features are not cell-type dependent but could be a characteristic of HGSOC with CBP-induced AMP. Our data indicate that acquired change in the expression of miR-103a–3p impacts metastatic potential but not drug response of HGSOC cells even though the stress inducer is the same, implying separate regulation of these two phenomena in the context of this specific miRNA.

Since the high mortality of OC results mostly from the development of metastases [66], we were further interested in exploring whether the selected miRNAs have prognostic value regarding the cancer types with similar characteristics as our cell model, showing a decrease in expression of several markers of stem-like phenotype. Indeed, the miR-103a–3p and miR-107, but not miR-17–5p, have prognostic value for all OC patients, especially those with enriched mesenchymal stem cells. Additionally, prognostic values of three miRNAs were confirmed in 18 different tumors, while their expression values were unable to predict the survival of patients with Esophageal Squamous Cell Carcinoma, Pheochromocytoma, Paraganglioma and Rectum adenocarcinoma. According to known data, it seems that miR-103a and miR-107 could be interesting markers of the OC therapy response [67], but further research is needed regarding their functional role.

In conclusion, here we showed how CBP-induced epigenetic modulation of miRNA expression influences pathways involved in cell invasion. This study confirms the importance of epigenetic modifications in the regulation of the metastatic capacity of cancer cells with acquired drug-induced mesenchymal-like phenotype. More importantly, it shows that the combination of miRNA and mRNA profiling of CBP-resistant OC cell model, selection of epigenetically regulated miRNAs, and further selection in other drug-resistant, mesenchymal-like cancer cell lines is a valuable tool for finding possible regulators of drug-induced metastatic potential and prognostic markers. Future research is needed to elucidate signaling pathways behind described regulations and the complexity of their interconnection and to determine in more detail which molecules are possible connectors of drug resistance and drug-induced mesenchymal-like phenotype and which regulate these two phenomena separately.

Funding

This study was supported by the Croatian Science Foundation (CSF, project number IP-2016-06-1036 and DOK-2018-01-8086), the Croatian-Austrian bilateral project supported by the Ministry of Science and Education of the Republic of Croatia and the Austrian Agency for International Cooperation in Education and Research, the Prometheus Fund-Foundation of the University of Rijeka and the large-scale Croatian-Chinese project supported by the Ministry of Science and Education of the Republic of Croatia and Ministry of Science and Technology of the People's Republic of China.

CRediT authorship contribution statement

Margareta Pernar Kovač: Conceptualization, Investigation, Writing – original draft, Writing – review & editing. **Vanja Tadić:** Conceptualization, Investigation, Writing – review & editing. **Juran Kralj:** Conceptualization, Investigation, Writing – review & editing. **Marija Milković Periša:** Writing – review & editing. **Slavko Orešković:** Writing – review & editing. **Vladimir Banović:** Writing – review & editing. **Ivan Babić:** Writing – review & editing. **Wei Zhang:** Funding acquisition, Writing – review & editing. **Zoran Culig:** Funding acquisition, Writing – review & editing. **Anamaria Brozovic:** Conceptualization, Investigation, Supervision, Funding acquisition, Project administration, Writing – original draft, Writing – review & editing.

Declaration of Competing Interest

The authors declare that there are no conflicts of interest.

Data Availability

Data will be made available on request. All data supporting the findings of this study are included within the article and its Supplementary Information files. Also, the data will be shared upon reasonable request to the corresponding author from colleagues who want to analyze in deep our findings.

Acknowledgments

The authors would like to thank BSc Matej Kovač for the help regarding big data analysis and Mag. Biotech. Marina Šutalo (Ruđer Bošković Institute) for technical assistance. The authors would also like to thank Marija Klasić, PhD (Faculty of Science, University of Zagreb) for invaluable input and technical advice with chromatin analysis.

Appendix A. Supporting information

Supplementary data associated with this article can be found in the online version at doi:10.1016/j.biopha.2023.115349.

References

[1] A. Gadducci, V. Guarneri, F.A. Peccatori, G. Ronzino, G. Scandurra, C. Zamagni, P. Zola, V. Salutari, Current strategies for the targeted treatment of high-grade serous epithelial ovarian cancer and relevance of BRCA mutational status, J. Ovarian Res. 12 (2019) 9.
[2] D. Jelovac, D.K. Armstrong, Recent progress in the diagnosis and treatment of ovarian cancer, CA Cancer J. Clin. 61 (2011) 183–203.
[3] E. Smolle, V. Taucher, J. Haybaeck, Malignant ascites in ovarian cancer and the role of targeted therapeutics, Anticancer Res. 34 (2014) 1553–1561.
[4] A. Brozovic, The relationship between platinum drug resistance and epithelial-mesenchymal transition, Arch. Toxicol. 91 (2017) 605–619.
[5] N. Erin, J. Grahovac, A. Brozovic, T. Efferth, Tumor microenvironment and epithelial mesenchymal transition as targets to overcome tumor multidrug resistance, Drug Resist Updat 53 (2020), 100715.
[6] T. Shibue, R.A. Weinberg, EMT, CSCs, and drug resistance: the mechanistic link and clinical implications, Nat. Rev. Clin. Oncol. 14 (2017) 611–629.
[7] S. Khan, H. Ayub, T. Khan, F. Wahid, MicroRNA biogenesis, gene silencing mechanisms and role in breast, ovarian and prostate cancer, Biochimie 167 (2019) 12–24.
[8] P.M. Voorhoeve, MicroRNAs: Oncogenes, tumor suppressors or master regulators of cancer heterogeneity? Biochim. Biophys. Acta 1805 (2010) 72–86.
[9] K. Zhou, M. Liu, Y. Cao, New insight into microRNA functions in cancer: oncogene-microRNA-tumor suppressor gene network, Front. Mol. Biosci. 4 (2017) 46.
[10] Q. Yao, Y. Chen, X. Zhou, The roles of microRNAs in epigenetic regulation, Curr. Opin. Chem. Biol. 51 (2019) 11–17.

[11] V. Davalos, C. Moutinho, A. Villanueva, R. Boque, P. Silva, F. Carneiro, M. Esteller, Dynamic epigenetic regulation of the microRNA-200 family mediates epithelial and mesenchymal transitions in human tumorigenesis, Oncogene 31 (2012) 2062–2074.
[12] A. Brozovic, G.E. Duran, Y.C. Wang, E.B. Francisco, B.I. Sikic, The miR-200 family differentially regulates sensitivity to paclitaxel and carboplatin in human ovarian carcinoma OVCAR-3 and MES-OV cells, Mol. Oncol. 9 (2015) 1678–1693.
[13] W. Xie, H. Sun, X. Li, F. Lin, Z. Wang, X. Wang, Ovarian cancer: epigenetics, drug resistance, and progression, Cancer Cell Int. 21 (2021) 434.
[14] K. Chen, M.X. Liu, C.S. Mak, M.M. Yung, T.H. Leung, D. Xu, S.F. Ngu, K.K. Chan, H. Yang, H.Y. Ngan, D.W. Chan, Methylation-associated silencing of miR-193a-3p promotes ovarian cancer aggressiveness by targeting GRB7 and MAPK/ERK pathways, Theranostics 8 (2018) 423–436.
[15] V.I. Loginov, I.V. Pronina, A.M. Burdennyy, E.A. Filippova, T.P. Kazubskaya, D. N. Kushlinsky, D.O. Utkin, D.S. Khodyrev, N.E. Kushlinskii, A.A. Dmitriev, E. A. Braga, Novel miRNA genes deregulated by aberrant methylation in ovarian carcinoma are involved in metastasis, Gene 662 (2018) 28–36.
[16] J. Kralj, M. Pernar Kovac, S. Dabelic, D.S. Polancec, T. Wachtmeister, K. Kohrer, A. Brozovic, Transcriptome analysis of newly established carboplatin-resistant ovarian cancer cell model reveals genes shared by drug resistance and drug-induced EMT, Br. J. Cancer 128 (2023) 1344–1359.
[17] J. O'Brien, I. Wilson, T. Orton, F. Pognan, Investigation of the Alamar Blue (resazurin) fluorescent dye for the assessment of mammalian cell cytotoxicity, Eur. J. Biochem 267 (2000) 5421–5426.
[18] A. Kozomara, M. Birgaoanu, S. Griffiths-Jones, miRBase: from microRNA sequences to function, Nucleic Acids Res. 47 (2019) D155–D162.
[19] W.J. Kent, C.W. Sugnet, T.S. Furey, K.M. Roskin, T.H. Pringle, A.M. Zahler, D. Haussler, The human genome browser at UCSC, Genome Res. 12 (2002) 996–1006.
[20] K.R. Rosenbloom, C.A. Sloan, V.S. Malladi, T.R. Dreszer, K. Learned, V.M. Kirkup, M.C. Wong, M. Maddren, R. Fang, S.G. Heitner, B.T. Lee, G.P. Barber, R.A. Harte, M. Diekhans, J.C. Long, S.P. Wilder, A.S. Zweig, D. Karolchik, R.M. Kuhn, D. Haussler, W.J. Kent, ENCODE data in the UCSC genome browser: year 5 update, Nucleic Acids Res. 41 (2013) D56–D63.
[21] D. Karolchik, A.S. Hinrichs, T.S. Furey, K.M. Roskin, C.W. Sugnet, D. Haussler, W. J. Kent, The UCSC Table Browser data retrieval tool, Nucleic Acids Res. 32 (2004) D493–D496.
[22] L.C. Li, R. Dahiya, MethPrimer: designing primers for methylation PCRs, Bioinformatics 18 (2002) 1427–1431.
[23] K.H. Lee, C. Lotterman, C. Karikari, N. Omura, G. Feldmann, N. Habbe, M. G. Goggins, J.T. Mendell, A. Maitra, Epigenetic silencing of microRNA miR-107 regulates cyclin-dependent kinase 6 expression in pancreatic cancer, Pancreatology 9 (2009) 293–301.
[24] C. Sticht, C. De La Torre, A. Parveen, N. Gretz, miRWalk: an online resource for prediction of microRNA binding sites, PLoS One 13 (2018), e0206239.
[25] A. Majchrzak-Celinska, A. Warych, M. Szoszkiewicz, Novel approaches to epigenetic therapies: from drug combinations to epigenetic editing, Genes 12 (2021).
[26] A. Nagy, G. Munkacsy, B. Gyorffy, Pancancer survival analysis of cancer hallmark genes, Sci. Rep. 11 (2021) 6047.
[27] D.S. Chandrashekar, B. Bashel, S.A.H. Balasubramanya, C.J. Creighton, I. Ponce-Rodriguez, B. Chakravarthi, S. Varambally, UALCAN: a portal for facilitating tumor subgroup gene expression and survival analyses, Neoplasia 19 (2017) 649–658.
[28] J.T. Fekete, B. Gyorffy, ROCplot.org: Validating predictive biomarkers of chemotherapy/hormonal therapy/anti-HER2 therapy using transcriptomic data of 3,104 breast cancer patients, Int. J. Cancer 145 (2019) 3140–3151.
[29] G.E. Duran, Y.C. Wang, F. Moisan, E.B. Francisco, B.I. Sikic, Decreased levels of baseline and drug-induced tubulin polymerisation are hallmarks of resistance to taxanes in ovarian cancer cells and are associated with epithelial-to-mesenchymal transition, Br. J. Cancer 116 (2017) 1318–1328.
[30] F. Moisan, E.B. Francisco, A. Brozovic, G.E. Duran, Y.C. Wang, S. Chaturvedi, S. Seetharam, L.A. Snyder, P. Doshi, B.I. Sikic, Enhancement of paclitaxel and carboplatin therapies by CCL2 blockade in ovarian cancers, Mol. Oncol. 8 (2014) 1231–1239.
[31] N. Wajapeyee, R. Gupta, Epigenetic alterations and mechanisms that drive resistance to targeted cancer therapies, Cancer Res. 81 (2021) 5589–5595.
[32] K.M.T. Arif, E.K. Elliott, L.M. Haupt, L.R. Griffiths, Regulatory mechanisms of epigenetic miRNA relationships in human cancer and potential as therapeutic targets, Cancers 12 (2020).
[33] H. Suzuki, S. Takatsuka, H. Akashi, E. Yamamoto, M. Nojima, R. Maruyama, M. Kai, H. Yamano, Y. Sasaki, T. Tokino, Y. Shinomura, K. Imai, M. Toyota, Genome-wide profiling of chromatin signatures reveals epigenetic regulation of microRNA genes in colorectal cancer, Cancer Res. 71 (2011) 5646–5658.
[34] X.L. Liu, X.Y. Chen, X.F. Yu, Y.G. Tao, A.M. Bode, Z.G. Dong, Y. Cao, Regulation of microRNAs by epigenetics and their interplay involved in cancer, J. Exp. Clin. Cancer Res. 32 (2013) 96.
[35] T. Kunej, I. Godnic, J. Ferdin, S. Horvat, P. Dovc, G.A. Calin, Epigenetic regulation of microRNAs in cancer: an integrated review of literature, Mutat. Res-Fund. Mol. 717 (2011) 77–84.
[36] S.P. Kabekkodu, V. Shukla, V.K. Varghese, D. Adiga, P. Vethil Jishnu, S. Chakrabarty, K. Satyamoorthy, Cluster miRNAs and cancer: diagnostic, prognostic and therapeutic opportunities, Wiley Inter. Rev. RNA 11 (2020), e1563.
[37] J. Wang, M. Haubrock, K.M. Cao, X. Hua, C.Y. Zhang, E. Wingender, J. Li, Regulatory coordination of clustered microRNAs based on microRNA-transcription factor regulatory network, BMC Syst. Biol. 5 (2011) 199.
[38] Y. Ma, N. Shen, M.S. Wicha, M. Luo, The roles of the let-7 family of microRNAs in the regulation of cancer stemness, Cells 10 (2021) 2415.
[39] G. Pan, Y. Liu, L. Shang, F. Zhou, S. Yang, EMT-associated microRNAs and their roles in cancer stemness and drug resistance, Cancer Commun. 41 (2021) 199–217.
[40] Y. Ruike, A. Ichimura, S. Tsuchiya, K. Shimizu, R. Kunimoto, Y. Okuno, G. Tsujimoto, Global correlation analysis for micro-RNA and mRNA expression profiles in human cell lines, J. Hum. Genet. 53 (2008) 515.
[41] D.W. Huang, B.T. Sherman, Q. Tan, J.R. Collins, W.G. Alvord, J. Roayaei, R. Stephens, M.W. Baseler, H.C. Lane, R.A. Lempicki, The DAVID gene functional classification tool: a novel biological module-centric algorithm to functionally analyze large gene lists, Genome Biol. 8 (2007) R183.
[42] D.W. Huang, B.T. Sherman, Q. Tan, J. Kir, D. Liu, D. Bryant, Y. Guo, R. Stephens, M.W. Baseler, H.C. Lane, R.A. Lempicki, DAVID bioinformatics resources: expanded annotation database and novel algorithms to better extract biology from large gene lists, Nucleic Acids Res. 35 (2007) W169–W175.
[43] T.H. Beacon, G.P. Delcuve, C. Lopez, G. Nardocci, I. Kovalchuk, A.J. van Wijnen, J. R. Davie, The dynamic broad epigenetic (H3K4me3, H3K27ac) domain as a mark of essential genes, Clin. Epigenet. 13 (2021) 138.
[44] M.P. Creyghton, A.W. Cheng, G.G. Welstead, T. Kooistra, B.W. Carey, E.J. Steine, J. Hanna, M.A. Lodato, G.M. Frampton, P.A. Sharp, L.A. Boyer, R.A. Young, R. Jaenisch, Histone H3K27ac separates active from poised enhancers and predicts developmental state, Proc. Natl. Acad. Sci. USA 107 (2010) 21931–21936.
[45] N. Ahmed, K. Abubaker, J. Findlay, M. Quinn, Epithelial mesenchymal transition and cancer stem cell-like phenotypes facilitate chemoresistance in recurrent ovarian cancer, Curr. Cancer Drug Targets 10 (2010) 268–278.
[46] J. Pijuan, C. Barcelo, D.F. Moreno, O. Maiques, P. Siso, R.M. Marti, A. Macia, A. Panosa, *In vitro* cell migration, invasion, and adhesion assays: from cell imaging to data analysis, Front. Cell Dev. Biol. 7 (2019) 107.
[47] C.Y. Yen, H.W. Huang, C.W. Shu, M.F. Hou, S.S.F. Yuan, H.R. Wang, Y.T. Chang, A. A. Farooqi, J.Y. Tang, H.W. Chang, DNA methylation, histone acetylation and methylation of epigenetic modifications as a therapeutic approach for cancers, Cancer Lett. 373 (2016) 185–192.
[48] M.S. Anglesio, K.C. Wiegand, N. Melnyk, C. Chow, C. Salamanca, L.M. Prentice, J. Senz, W. Yang, M.A. Spillman, D.R. Cochrane, K. Shumansky, S.P. Shah, S. E. Kalloger, D.G. Huntsman, Type-specific cell line models for type-specific ovarian cancer research, PLoS One 8 (2013), e72162.
[49] J. O'Brien, H. Hayder, Y. Zayed, C. Peng, Overview of microRNA biogenesis, mechanisms of actions, and circulation, Front. Endocrinol. (Lausanne) 9 (2018) 402.
[50] A. Appert-Collin, P. Hubert, G. Cremel, A. Bennasroune, Role of ErbB receptors in cancer cell migration and invasion, Front. Pharm. 6 (2015) 283.
[51] E. Castellano, M. Molina-Arcas, A.A. Krygowska, P. East, P. Warne, A. Nicol, J. Downward, RAS signalling through PI3-Kinase controls cell migration via modulation of Reelin expression, Nat. Commun. 7 (2016) 11245.
[52] Y. Zhang, S. Kwon, T. Yamaguchi, F. Cubizolles, S. Rousseaux, M. Kneissel, C. Cao, N. Li, H.L. Cheng, K. Chua, D. Lombard, A. Mizeracki, G. Matthias, F.W. Alt, S. Khochbin, P. Matthias, Mice lacking histone deacetylase 6 have hyperacetylated tubulin but are viable and develop normally, Mol. Cell Biol. 28 (2008) 1688–1701.
[53] Y. Watanabe, M. Koi, H. Hemmi, H. Hoshai, K. Noda, A change in microsatellite instability caused by cisplatin-based chemotherapy of ovarian cancer, Br. J. Cancer 85 (2001) 1064–1069.
[54] E. Mogilyansky, I. Rigoutsos, The miR-17/92 cluster: a comprehensive update on its genomics, genetics, functions and increasingly important and numerous roles in health and disease, Cell Death Differ. 20 (2013) 1603–1614.
[55] G. Zhang, Z. Chen, Y. Zhang, T. Li, Y. Bao, S. Zhang, Inhibition of miR-103a–3p suppresses the proliferation in oral squamous cell carcinoma cells via targeting RCAN1, Neoplasma 67 (2020) 461–472.
[56] H. Li, M. Huhe, J. Lou, MicroRNA-103a-3p promotes cell proliferation and invasion in non-small-cell lung cancer cells through Akt pathway by targeting PTEN, Biomed. Res. Int. 2021 (2021) 7590976.
[57] G.Z. Zhao, Z.L. Wei, Y. Guo, MicroRNA-107 is a novel tumor suppressor targeting POU3F2 in melanoma, Biol. Res. 53 (2020) 11.
[58] H. Xia, Y. Li, X.H. Lv, MicroRNA-107 inhibits tumor growth and metastasis by targeting the BDNF-mediated PI3K/AKT pathway in human non-small lung cancer, Int J. Oncol. 49 (2016) 1325–1333.
[59] N.M. Novikov, S.Y. Zolotaryova, A.M. Gautreau, E.V. Denisov, Mutational drivers of cancer cell migration and invasion, Br. J. Cancer 124 (2021) 102–114.

[60] Z. Tang, Y. Fang, R. Du, MicroRNA-107 induces cell cycle arrests by directly targeting cyclin E1 in ovarian cancer, Biochem. Biophys. Res. Commun. 512 (2019) 331–337.
[61] A.A. Jiao, F.J. Slack, MicroRNAs micromanage themselves, Circ. Res. 111 (2012) 1395–1397.
[62] H.Y. Jin, A. Gonzalez-Martin, A.V. Miletic, M.Y. Lai, S. Knight, M. Sabouri-Ghomi, S.R. Head, M.S. Macauley, R.C. Rickert, C.C. Xiao, Transfection of microRNA mimics should be used with caution, Front. Genet. 6 (2015) 340.
[63] P.M.D. Costa, S.L.A. Sales, D.P. Pinheiro, L.Q. Pontes, S.S. Maranhao, C.D. Pessoa, G.P. Furtado, C.L.M. Furtado, Epigenetic reprogramming in cancer: from diagnosis to treatment, Front. Cell Dev. Biol. 11 (2023) 1116805.
[64] H. Yang, P. Lan, Z. Hou, Y. Guan, J. Zhang, W. Xu, Z. Tian, C. Zhang, Histone deacetylase inhibitor SAHA epigenetically regulates miR-17-92 cluster and MCM7 to upregulate MICA expression in hepatoma, Br. J. Cancer 112 (2015) 112–121.
[65] L.F. Gulyaeva, N.E. Kushlinskiy, Regulatory mechanisms of microRNA expression, J. Transl. Med. 14 (2016) 143.
[66] T. Motohara, K. Masuda, M. Morotti, Y. Zheng, S. El-Sahhar, K.Y. Chong, N. Wietek, A. Alsaadi, E.M. Carrami, Z. Hu, M. Artibani, L.S. Gonzalez, H. Katabuchi, H. Saya, A.A. Ahmed, An evolving story of the metastatic voyage of ovarian cancer cells: cellular and molecular orchestration of the adipose-rich metastatic microenvironment, Oncogene 38 (2019) 2885–2898.
[67] R. Di Fiore, S. Suleiman, F. Pentimalli, S.A. O'Toole, J.J. O'Leary, M.P. Ward, N. T. Conlon, M. Sabol, P. Ozretic, A.E. Erson-Bensan, N. Reed, A. Giordano, C. S. Herrington, J. Calleja-Agius, Could microRNAs be useful tools to improve the diagnosis and treatment of rare gynecological cancers? A brief overview, Int. J. Mol. Sci. 22 (2021).